Delft University of Technology

Improved Grid Reliability by Robust Distortion Detection and Classification Algorithm

Bhandia, Rishabh; Cvetkovic, Milos; Palensky, Peter

Improved Grid Reliability by Robust Distortion Detection and Classification Algorithm

Rishabh Bhandia*, Miloš Cvetković, Peter Palensky
Department of Electrical Sustainable Energy
Delft University of Technology, Delft, The Netherlands
*email: r.bhandia@tudelft.nl

Abstract— **Deviations from normal power grid operations, such as incipient faults, equipment damage, or weather related effects, have characteristic signatures in the current and voltage waveforms. Detecting and classifying such signal distortions as quick as possible can contribute to grid reliability since grid events can be responded to in time, i.e. before they lead to an outage. This paper proposes a new distortion detection algorithm, based on computationally very lightweight operations. The method does not require large datasets, has a small memory footprint, and therefore can be easily implemented on decentralized, embedded systems. This detection method constitutes the core of an overarching algorithm which accurately classifies the event even in case of a malfunctioning device and normal switching action. The paper investigates the performance of this new algorithm and evaluates it with four case studies for High Impedance Faults occurring on a IEEE 9 bus system.**

Index Terms-- **power system reliability, waveform analytics, high impedance fault , distortion detection, power system protection.**

I. INTRODUCTION

Today's power system has become more complex with implementation and integration of new technologies. These new technologies have transformed the conventional behavioral pattern in all domains of the power system like generation, transmission, control, storage etc. This change has necessitated the need for improved monitoring schemes to assess the reliable working of the grid at all times. The advent of newer technology has led to the availability of efficient and high-fidelity measurement devices like Advanced Metering Initiative (AMI), Phasor Measurement Unit (PMU) and other intelligent electrical devices [1], [2]. These high fidelity measuring devices have made it feasible to record waveforms with greater precision and higher sampling rates. The intelligent electrical devices discussed above are constantly monitoring the grid leading to generation of large amounts of data every second. This grid data is very valuable as they contain vital information about the grid's operation but the huge volume of data imposes a big challenge to efficiently process and extract useful information from it. When the grid data is processed effectively, it will give significant information, which can be used to protect the grid from harmful events.

Harmful events like faults or any other similar disturbance, can negatively affect the normal operation of the grid. The consequences of large-scale power outages are substantial financial loss and inconvenience to the consumers. Classical electrical protection schemes and devices come into action after a fault or a similar event has taken place. Sometimes these procedures are not enough or too late, leading to extensive outages and equipment damage [3]. The perception in general in the power industry is that a normally working power grid is considered healthy until a fault or a similar disturbance occurs leading to the collapse of the grid.

However, in real life, typically there exists a *pre-failure period*. A pre-failure period can be defined as a time interval between the normal operating conditions of the grid and its subsequent collapse [1]. The pre-failure time period can range from few minutes to few weeks or even few months. In this period the grid, though stable, is enduring more stress than normal. It is during this pre-failure period that incipient faults, partially damaged equipment or adverse weather conditions leave behind their signatures in form of distortions in the otherwise pure sinusoid AC current/ voltage waveforms. The time interval of the pre-failure period is the window of opportunity where we utilize waveform analytics to analyze the measured waveforms to detect and classify a potentially harmful event for the grid. Timely detection and classification of the distortions can protect the grid from extensive outages.

There are existing studies, where waveform analytics have been used to improve the reliability of the grid. Electrical Power Research Institute (EPRI) along with Texas A&M University has developed a tool to detect and classify failures on a distribution system [3]. In [4] and [5], they show how tool relies on the massive database created by electrical waveforms recorded from failing electrical devices while in [6], the damage due to non-technical loss has been tackled using artificial intelligence. Wavelet transformations have been used for detection and classification of power quality disturbances [7], [8]. In [9] and[10], wavelet transformation has been combined with neural networks to detect and classify power disturbance events. The techniques discussed above

require a large database of fault signatures which involve considerable startup resource cost. Additionally, in techniques involving neural networks, considerable memory and computing power is needed.

This paper proposes a new distortion detection technique to improve the reliability of the grid. This distortion detection technique forms the core of a larger algorithm that further processes the detected distortions in order to classify the nature of the event (harmful/not harmful) causing the distortion. The classification information is relayed to the operator who can then take appropriate actions to maintain the reliability of the grid. The distortion detection technique leverages the sinusoid nature of voltage and current waveforms in the AC grid as explained in the subsequent sections. The wavelet transform based techniques involve breaking the waveform into high and low frequency transients before analysis of the waveform can be started. The distortion detection technique does not refer to any database to detect a distortion and analyses the waveforms continuously online which makes the technique unique and much. The mathematical backbone of the distortion detection technique is a simple yet robust difference based approach which does not require large memory or huge computing power. A similar difference based waveform analytics approach has been used for current transformer saturation detection and compensation in [11]. The proposed distortion detection and classification function algorithm can be used for anticipation of faults, diagnosis of failure in the power system and for detecting faults where the conventional protection systems have shown weaker results like in the case of High Impedance Fault (HIF) [12]-[14]. Hence, the proposed algorithm acts as an early warning system for a possible outage in the system.

We validate the algorithm by conducting simulations in real-time using the Real Time Digital Simulator (RTDS) facility. The paper presents an example simulation with five different case studies to show the robustness of the algorithm. The example simulation shows an HIF on an IEEE 9 bus system designed in the RSCAD software.

The paper has been structured as following: Section II discusses the mathematics behind the distortion detection technique that forms the core part of the proposed algorithm. Section III describes in detail the principle of the entire algorithm including the classification criteria. Section IV presents and discusses the simulation results obtained when the algorithm is applied on the four example use cases. Finally, Section V presents the conclusions.

II. DISTORTION DETECTION AS A DIFFERENCE FUNCTION

In this section, we discuss the distortion detection technique in detail and outline how it can be constructed as a difference function. The current and voltage waveforms in an AC power system are sinusoid and can be described as complex exponentials using Euler formula as seen in (1):

$$e^{j\omega t} = \cos \omega t + j \sin \omega t \qquad (1)$$

where ω is the angular frequency (*in radians per second*), t is time (*seconds*) and j is the imaginary unit.

An exponential function has one distinct characteristic, the rate of increase or decrease of an exponential function is proportional to the value of the function at that instant. An added characteristic of a complex exponential function is that it is not infinitely increasing or decreasing. The complex exponential function rotates around the unit circle in a complex plane. These characteristics of the complex exponential functions are used for devising the difference based distortion detection technique. In particular, the technique compares the values of the first difference of a measured signal and ensures that these values trace the line of the complex exponential function.

The distortion detection technique proposed in this paper uses the first difference instead of continuous differentials since the signals that are being processed are sampled voltages and current in the power grid. Mathematical formulation of the previously illustrated concept is presented next.
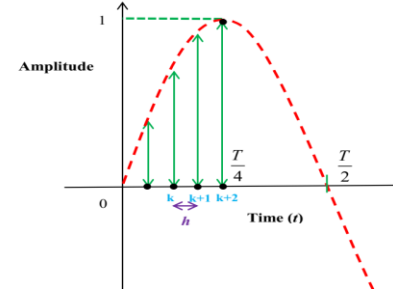

Figure 1. Sampled signal $f[k]$

The sampled signal $f[k]$, as shown in Fig. 1 is a general representation of any voltage or current signal measured from the grid. Assuming the signal as a sine wave of period T, which can be sampled at N samples per cycle, the samples could be denoted as: $n...k, k+1, k+2...n+N$. The samples are equally spaced in time-domain at an interval of length h, such that:

$$T = h.N \qquad (2)$$

Let $g[k]$ be the difference of the sample values at sample k and $k+1$, the first difference at k can be written as:

$$g[k] = \frac{f[k]-f[k-1]}{h} \qquad (3)$$

Similarly at $k+1$:

$$g[k+1] = \frac{f[k+1]-f[k]}{h} \qquad (4)$$

Now, for a pure sine wave, using (3) and (4), it can be written that:

$$g[k] > g[k+1], k \in \left\{n, n+\frac{T}{4}\right\} \cup \left\{n+\frac{T}{2}, n+\frac{3T}{4}\right\} \quad (5)$$

$$g[k] < g[k+1], k \in \left\{n+\frac{T}{4}, n+\frac{T}{2}\right\} \cup \left\{n+\frac{3T}{4}, n+T\right\} \quad (6)$$

Hence if $f[k]$ is a pure sine wave, (5) and (6) will always hold true. In case, (5) or (6) are violated, the violation will be

recorded as a distortion. The violation will be interpreted as a distortion as for that instant, $f[k]$, would cease to be a pure sine wave.

III. DISTORTION DETECTION AND CLASSIFICATION ALGORITHM

In this section, we discuss the detection and classification algorithm in detail. The illustration of the algorithm is presented in Fig. 2. This section explains how the measured electrical waveforms are analyzed and classified. The four major blocks of the algorithm are Distortion Detection, Distortion Recorder, Synchronizer and Classifier. We discuss them in detail in this section.

A. Distortion Detection

The mathematics governing the Distortion Detection technique has been explained in the previous section. The main objective of this block is to implement the distortion detection technique. The input to this block is current or voltage waveform $f[k]$, measured with a sampling rate R from a particular node in the grid. Whenever this block
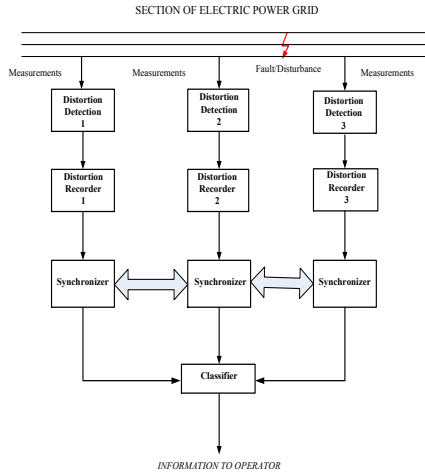

Figure 2. Algorithm Flowchart
(The input and output of each block is explained in the main text)

detects violation of (5) or (6), a flag is raised and distortion reported. The output of this block is (d, t) where d indicates the occurrence of the distortion at time t. We can define d as, $d = 1$, if distortion is detected and $d = 0$, if distortion is not detected. The output of this block serves as an input to the Distortion Recorder block.

B. Distortion Recorder

The objective of this block is to store the distortion occurrence data from Distortion Detection block in a data set of a specified length as explained below. This data set is called Memory Buffer. The input to this block is (d, t). The input data is collected and processed by an N sample window as it moves along the entire waveform. The size of the window is user-dependent and could vary from one

measuring device to another. If we have m measuring devices such that $i = 1, 2, 3...m$, then the memory buffer W_i in the time interval of (a_i, b_i) can be represented as:

$$W_i = \{(d_f, t_f) | d_f \in \{0,1\}, t_f \in (a_i, b_i), f = (1,2,3 \dots N)\}$$
(7)

The memory buffer W_i contains the instants of occurrence and non-occurrence of distortions in a fixed length of time interval (a_i, b_i). Eq. (7) is the output from the distortion recorder block and serves as an input to the synchronizer block.

C. Synchronizer

The main objective of this block is the synchronization of all the data received from the distortion recorder block. The synchronization helps in aligning all the reported distortions such that a correct classification can be achieved. If not, it will cause false flag error leading to wrong results. The occurrence of a disturbance at a certain point in the grid will not have the same impact over the entire section of the grid. For the same distortion, some measurement devices may report numerous and frequent distortion levels, some lower and some may not report any distortion at all. Also, the measurement devices may not have uniform sampling rates. For synchronization, comparison and further analysis of the distortion detection data we need a window of fixed time interval to collect all reporting's from different measurement devices during that time interval. The device with the highest sampling rate will report maximum distortion detection data in that fixed time interval compared to other measurement devices. Hence, the base window is integer-proportional to the size of the reporting time interval of the highest sampling measurement device. The base window A can be represented as:

$$A = (a_{base}, b_{base}) = \bigcap_{i=1}^{n} (a_i, b_i) \quad (8)$$

The curtailed memory buffer, $\widetilde{W}_i$, within the size limits of the base window can be represented as:

$$\widetilde{W}_i = \{w_i = (d_f, t_f) | w_i \text{ and } t_f \in (a_{base}, b_{base}) \text{ and } d_f \in \{0,1\}\}$$
(9)

The last processing step of this block is to sum the values of the distortion occurrences d_f in $\widetilde{W}_i$. We can write:

$$C_i = \sum_{p=1}^{|\widetilde{W}_i|} d_p$$
(10)

Thus, (10) is the output from each synchronizer block sent to the classifier.

D. Classifier

As the name suggests, the main objective of this block is to classify events and present the output to the operator. The classifier classifies the event as either *'not harmful'* or *'potentially harmful'*. The classifier performs two main functions to classify any event causing distortion. The two functions are analysis of the reported distortions per

measuring device and analysis of the reported distortions over the entire set of measuring devices:

1) Reported distortions per device

The first function is to check the number of distortions occurring in each curtailed memory buffer $\overline{W}_t$. The value of C_i for each synchronizer block is compared against a threshold th_i. If $C_i > th_i$, a flag is raised, else the classifier doesn't process it further. The value of the threshold is empirically chosen. In our case study, it was chosen based on the comparison between the number of distorted samples recorded during a non-harmful event like switching actions and a harmful event like HIF. The logic behind this function is based on observations that a normal switching event might result in a small distortion of signal but the impact will be reflected on one or two samples and it will not repeat itself. Such an event will not exceed the threshold and trigger a warning unnecessarily. However a disturbance leading to a fault or an equipment failure would result in numerous and repeated distortions throughout the waveform, due to which the threshold limit value would be exceeded multiple times and a warning would be triggered. Both these examples have been further analyzed in the presented case studies.

2) Number of devices reporting distortions

The other function of the classifier block is to check the distortions reported from the waveforms recorded by all the measuring devices in a certain section of the grid. As the input to the classifier has already been synchronized, it is easier for classifier to compare the reported distortions across different devices in the same interval. A relatively stable switching event might not produce distortions in each section of the grid but a fault inducing disturbance would affect the entire grid and would produce distortions in all sections of the grid. An example of another added advantage of this analysis is reduction of error due to malfunctioning of the measurement device. The comparison of reported threshold violations over the entire measurement set ensures that false positives are minimized. This scenario has been further explained in our case studies.

IV. SIMULATION AND RESULTS

An example use case has been created to show the practical application of the algorithm and validate its effectiveness. A standard IEEE 9 bus system is used for simulation [15]. The 9-bus system has been designed in RSCAD software to be simulated in RTDS. A High Impedance Fault (HIF) is simulated on the system. HIF current is generally below 75A [16]. In the experiments conducted in our research, we adjust the fault impedance to keep the HIF current within limit. The 9-bus system has been designed in RSCAD software to be simulated in RTDS.

A. Simulation Setup

The simulation setup can be seen in Fig 3. The HIF has been simulated at the transmission line between bus 4 and bus 6 as a line to line fault. The measurement points (mp 1, mp 2, mp 3, mp 4, mp 5) record the waveforms sampled at 256 samples/cycle at five different locations as indicated in Fig 3. The HIF has been simulated by changing the fault impedance to a very high value at $t = 0.04s$, which will result in a very low fault current. Four different case studies have been simulated and the corresponding waveforms of interest shown in Fig. 4. In the first three case studies, an HIF fault has been implemented in different circumstances as explained further. The fourth case study illustrates the robustness of the algorithm with respect to switching actions. The result of the distortion detection and classification has been presented in Table I. The results shown in Table I is of most interest as it shows the reporting's by the algorithm just after the occurrence of the fault. An additional fifth case study has been conducted to assess the detection sensitivity of the proposed algorithm.

B. Case Studies

Case I *(Algorithm Validation)*:

In this case study, we validate the algorithm against an HIF event. The active measurement points are mp 1, mp 2 and mp 3. The measuring points mp4 and mp 5 are inactive. At the commencement of the fault, the waveforms at different
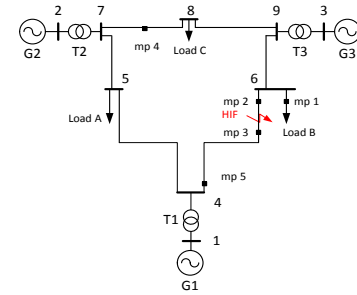

Figure 3. IEEE 9 bus system simulation setup

measuring points show distortion. As the fault current is low, the distortion at mp 1 is hardly visible to the naked eye as seen in Fig. 4(a), but the distortion detection technique detects it as seen in Table I. The event is further classified by the classifier as a potentially harmful event as repeated distortions have been reported by multiple Distortion Detection blocks over the same period of time. Hence, the algorithm is clearly able to identify an HIF.

Case II *(Realistic availability of measuring points)*:

In real-life it is not very economical to have measuring devices so close to each other as seen in Case I. Hence the setup in Case I might not be very practical. Case II aims to display the effectiveness of the algorithm in a more practical and real-life setup. The same HIF event is used in this case. The active measurement points are mp 3, mp 4 and mp 5. Measuring points mp 1 and mp 2 are inactive. As we can see from Fig. 4(b), the distortion at mp 4 (farthest from the fault location) is hardly visible but is detected by the distortion detection technique. As seen in Table I, varying extent of
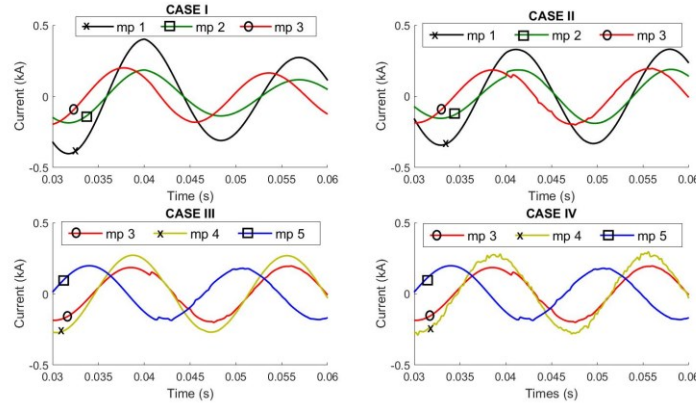
Figure 4. Comparison of current waveforms at different measuring points (mp) for different case studies.
(1)CASE I, (b) CASE II, (c) CASE III, (d) CASE IV

distortions detected above threshold are reported from different measurement points. The farthest measurement point reports the least distortions above threshold but it still accurately detects them during the interval of fault. This data is then processed through the algorithm, which relays the information to the operator that a potentially harmful event has occurred in the grid.

Case III *(Robustness to a malfunctioning measuring unit):*

It is a realistic possibility that a measuring device malfunctions due to ageing, physical damage or adverse weather effects. A typically malfunctioning measurement device might report erroneous results and distortions which actually did not occur. This can lead to error in judgement by the classifier. Case III is simulated in the same setup as of Case II. The measuring device at mp 4 is malfunctioning as seen in Fig 4(c). As observed from Table I, mp 4 reports random distortion detections that cross the threshold. However, the reported distortions are not entirely consistent with the distortion reports of the other two measuring points. As seen in Table I, due to monitoring at multiple measuring points, the erroneous reporting's of the malfunctioning device would be nullified and classifier would correctly detect the HIF. As the probability of all measuring units malfunctioning at the same time is comparatively rare, it can be said that the algorithm is immune to the effects of a random malfunctioning measurement device.

Case IV *(Robustness to false positives from switching transients):*

In this case study, we simulate a switching event in load B. The active power consumption of load B is varied by 10%. The active measurement points are mp 1, mp 2 and mp 3. Measuring points mp 4 and mp 5 are inactive. The results can be seen in Fig. 4(d). The switching event will lead to transients which would cause one or two sample distortions in the load current but not disrupt the reliable working of the grid. From the results in Table I, we see that the switching event did not result in violation of the threshold for any time period at any of the different measuring points. Hence, the classifier classifies it as a non-harmful event.

Case V *(Distortion Detection Sensitivity Analysis):*

In This case study we assess the detection sensitivity of the proposed algorithm to HIF current. The fault impedance is varied to simulate HIF currents between 0A to 75A. As defined before, maximum fault current in case of HIF doesn't generally exceed 75A. This low current value fails to trigger the relays and hence, HIF detection is still a considerable challenge for existing protection systems. The number of sample reporting distortion for each instance are recorded at different measurement points (mp 2, mp 4, mp 5). The result can be seen in Fig 5. We can see that even for very low fault current, there are some distortions reported at all measurement points. This displays the efficiency and wide applicability of the algorithm. Furthermore mp 4 being farthest from fault location shows least samples distorted while mp 2 being closest shows the highest samples distorted.
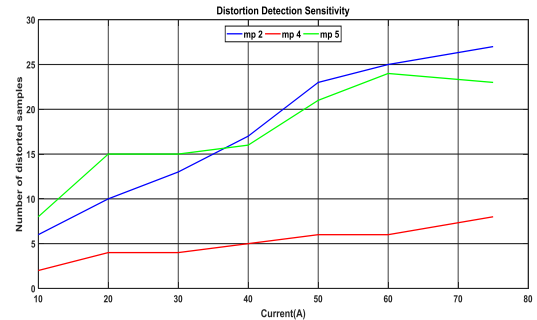

Figure 5. Distortion Detection sensitivity for different HIF current measuring points (mp) at different measurement points

V. CONCLUSIONS

In this paper we have developed a new distortion detection technique based on difference function which has not been previously used in this field. This detection technique along with other data processing blocks forms the distortion detection and classification algorithm. The effectiveness of the algorithm is successfully shown through presented case studies with HIF simulated on an IEEE 9 bus system. The case studies show the robustness and resiliency of the algorithm to false positives from effects of a malfunctioning measurement device and transients arising from switching actions. This lightweight yet robust algorithm

Table I
Distortion detection and classification results

Time Interval (s)	CASE I Distortions above threshold (Yes/No)			CASE II Distortions above threshold (Yes/No)			CASE III Distortions above threshold (Yes/No)			CASE IV Distortions above threshold (Yes/No)		
	MP 1	MP 2	MP 3	MP 3	MP 4	MP 5	MP 3	MP 4	MP 5	MP 1	MP 2	MP 3
0.0390-0.0398	No	No	No	No	No	No	No	Yes	No	No	No	No
0.0398-0.0406	Yes	Yes	No	No	No	No	No	No	No	No	No	No
0.0406-0.0414	**Yes**	**Yes**	**Yes**	Yes	No	Yes	Yes	Yes	No	No	No	No
0.0414-0.0422	**Yes**	**Yes**	**Yes**	**Yes**	**Yes**	**Yes**	**Yes**	No	**Yes**	No	No	No
0.0422-0.0430	**Yes**	**Yes**	**Yes**	**Yes**	**Yes**	**Yes**	**Yes**	No	**Yes**	No	No	No
0.0430-0.0438	**Yes**	**Yes**	**Yes**	**Yes**	**Yes**	**Yes**	**Yes**	Yes	**Yes**	No	No	No
0.0438-0.0446	Yes	No	No	No	Yes	No	No	No	No	No	No	No
0.0446-0.0454	No	No	No	No	No	No	No	Yes	No	No	No	No
CLASSFIER	**Potentially Harmful Event**			**Potentially Harmful Event**			**Potentially Harmful Event**			**No Harmful Event**		

can be easily implemented in the micro-controllers and can be used for smart monitoring of the power grid. Noise, harmonics are two major challenges to this algorithm and we are already working on it to make the algorithm more resilient. Cybersecurity is another major aspect of modern power systems which should be addressed to make the algorithm secure against malicious attacks. Future work will also involve modifying the distortion detection technique to record and analyze fast transients produced from events like lightning.

REFERENCES

[1] J. A. Wischkaemper, C. L. Benner, B. D. Russell and K. Manivannan, "Application of Waveform Analytics for Improved Situational Awareness of Electric Distribution Feeders," in *IEEE Transactions on Smart Grid*, vol. 6, no. 4, pp. 2041-2049, July 2015.

[2] R. Bhandia*, R. Albuquerque, R. Caire, N. Hadjsaid and D. Picault, "Adaptive Weighted Least Squares-Based Algorithm to Estimate Synchronized Measurements over Wide Frequency Range," in *CIRED 2015-The 23nd International Conference on Electricity Distribution*, June 2015.

[3] B. D. Russell and C. L. Benner, "Intelligent Systems for Improved Reliability and Failure Diagnosis in Distribution Systems," in *IEEE Transactions on Smart Grid*, vol. 1, no. 1, pp. 48-56, June 2010.

[4] B. D. Russell, C. L. Benner, R. M. Cheney, C. F. Wallis, T. L. Anthony and W. E. Muston, "Reliability improvement of distribution feeders through real-time, intelligent monitoring," *2009 IEEE Power & Energy Society General Meeting*, Calgary, AB, 2009, pp. 1-8.

[5] J. A. Wischkaemper, C. L. Benner, B. D. Russell and K. M. Manivannan, "Waveform analytics-based improvements in situational awareness, feeder visibility, and operational efficiency," *2014 IEEE PES T&D Conference and Exposition*, Chicago, IL, USA, 2014, pp. 1-5.

[6] P. Glauner, J. Meira, P. Valtchev, R. State and F. Bettinger, "The Challenge of Non-Technical Loss Detection using Artificial Intelligence: A Survey", International Journal of Computational Intelligence Systems (IJCIS), vol. 10, issue 1, pp. 760-775, 2017

[7] S. Santoso, E. J. Powers, W. M. Grady and P. Hofmann, "Power quality assessment via wavelet transform analysis," in *IEEE Transactions on Power Delivery*, vol. 11, no. 2, pp. 924-930, Apr 1996.

[8] C. H. Lin and M. C. Tsao, "Power quality detection with classification enhancible wavelet-probabilistic network in a power system," in *IEE Proceedings - Generation, Transmission and Distribution*, vol. 152, no. 6, pp. 969-976, 4 Nov. 2005.

[9] Zwe-Lee Gaing, "Wavelet-based neural network for power disturbance recognition and classification," in *IEEE Transactions on Power Delivery*, vol. 19, no. 4, pp. 1560-1568, Oct. 2004.

[10] F. Charfi, F. Sellami and K. Al-Haddad, "Fault Diagnostic in Power System Using Wavelet Transforms and Neural Networks," *2006 IEEE International Symposium on Industrial Electronics*, Montreal, Que., 2006, pp. 1143-1148.

[11] Yong Cheol Kang, Ui Jai Lim, Sang Hee Kang and P. A. Crossley, "Compensation of the distortion in the secondary current caused by saturation and remanence in a CT," in *IEEE Transactions on Power Delivery*, vol. 19, no. 4, pp. 1642-1649, Oct. 2004.

[12] C. J. Kim, B. D. Russell and K. Watson, "A parameter-based process for selecting high impedance fault detection techniques using decision making under incomplete knowledge," in *IEEE Transactions on Power Delivery*, vol. 5, no. 3, pp. 1314-1320, Jul 1990.

[13] A. E. Emanuel, D. Cyganski, J. A. Orr, S. Shiller and E. M. Gulachenski, "High impedance fault arcing on sandy soil in 15 kV distribution feeders: contributions to the evaluation of the low frequency spectrum," in *IEEE Transactions on Power Delivery*, vol. 5, no. 2, pp. 676-686, Apr 1990.

[14] A. R. Sedighi, M. R. Haghifam, O. P. Malik and M. H. Ghassemian, "High impedance fault detection based on wavelet transform and statistical pattern recognition," in *IEEE Transactions on Power Delivery*, vol. 20, no. 4, pp. 2414-2421, Oct. 2005.

[15] The Illinois Center for a Smarter Electric Grid (ICSEG), "WSCC 9-Bus System," *Power Cases*, [Accessed. March 1, 2018]. [Online]

[16] C. G. Wester, "High impedance fault detection on distribution systems," *1998 Rural Electric Power Conference Presented at 42nd Annual Conference*, St. Louis, MO, 1998, pp. c5-1-5.